Bistability and Molecular Switching for Semiquinone and Catechol Complexes of Cobalt. Studies on Redox Isomerism for the Bis(pyridine) Ether Series $Co(py_2X)(3,6\text{-}DBQ)_2$, X = O, S, Se, and Te

Ok-Sang Jung,*[,1a] Du Hwan Jo,[1a] Young-A Lee,[1a] Brenda J. Conklin,[1b] and Cortlandt G. Pierpont*[,1b]

Korea Institute of Science and Technology, Cheongryang, Seoul 130-650 Korea, and Department of Chemistry and Biochemistry, University of Colorado, Boulder, Colorado 80309

Received October 3, 1996[⊗]

Intramolecular electron transfer between $Co^{II}(SQ)$ and $Co^{III}(Cat)$ species has been investigated for the series of complexes $Co(py_2X)(3,6\text{-}DBQ)_2$, where 3,6-DBQ are semiquinonate and catecholate forms of 3,6-di-*tert*-butyl-1,2-benzoquinone and py_2X is bis(pyridine) ether and its heteroatomic analogs with X = S, Se, and Te. Transition temperature for Co(III)/Co(II) redox isomerism decreases in steps of approximately 30 K in toluene solution and in steps of 80 K in the solid state for the complexes with X = S, Se, Te. This appears to be primarily associated with an entropy increase that results from low-energy shifts in vibrational modes with increasing heteroatomic mass. Complexes containing py_2O have been isolated at room temperature in two charge distributions, $Co^{II}(py_2O)(3,6\text{-}DBSQ)_2$ and $Co^{III}(py_2O)(3,6\text{-}DBSQ)(3,6\text{-}DBCat)$. Crystallographic characterization on both forms of the complex [$Co^{II}(py_2O)(3,6\text{-}DBSQ)_2$, monoclinic, $P2_1/c$, $a = 11.0280(2)$ Å, $b = 30.2750(9)$ Å, $c = 12.1120(2)$ Å, $\beta = 113.490(2)°$, $V = 3708.7(1)$ Å^3, $Z = 4$, $R = 0.056$; $Co^{III}(py_2O)(3,6\text{-}DBSQ)(3,6\text{-}DBCat)$, monoclinic, $P2_1/n$, $a = 9.882(3)$ Å, $b = 20.915(5)$ Å, $c = 17.579(4)$ Å, $\beta = 91.57(2)°$, $V = 3632(2)$ Å^3, $Z = 4$, $R = 0.054$] has shown that the py_2O ligand adopts a planar structure for the Co(II) isomer that shifts to a folded, nonplanar structure with the smaller Co(III) ion. This structural change is responsible for hysteresis in the Co(III) → Co(II) and Co(II) → Co(III) electron transfer steps in the solid state. Optically induced shifts in charge distribution have been investigated using a low-energy polychromatic light source.

Introduction

There is currently active interest in the development of molecular electronic agents for use as photonic optical data storage media. Compounds of specific interest are molecular materials that exchange between stable or metastable states in response to an optical signal creating an addressable memory effect. Most research in this area has focused on conjugated organic molecules that undergo frequency-sensitive reversible bond-forming reactions. Recent reviews by Lehn and Irie have presented an overview of this research.[2,3] Reversible transformations of transition metal complexes offer potential for the design of inorganic or organometallic switches. Kahn has reported spin transition complexes of iron(II) that show thermal hysteresis,[4] and Gütlich has investigated optically induced spin transitions.[5] But, no metal complexes have been found that function with the ease and reversibility of the organic systems. Quinone functionalities appear as components in organic switches, and the coupled redox chemistry of quinones with transition metals may provide the basis for an organo-transition metal switch. Lehn and Harriman have studied a quinone-tethered form of $Ru(bpy)_3^{2+}$ as a system that may exhibit light-induced switching, but the charge-separated state that results from Ru(II) → Q electron transfer is short-lived.[6]

Several years ago we reported the equilibrium between Co(III) and Co(II) redox isomers of a complex containing semiquinonate (SQ) and catecholate (Cat) ligands derived from 3,5-di-*tert*-butyl-1,2-benzoquinone (3,5-DBBQ) (eq 1).[7]

$$Co^{III}(bpy)(3,5\text{-}DBSQ)(3,5\text{-}DBCat) \rightarrow Co^{II}(bpy)(3,5\text{-}DBSQ)_2 \quad (1)$$

In recent research this has been extended to include complexes containing a broad class of N-donor coligands and to complexes prepared with 3,6-DBBQ.[8,9] Equilibria occur in separate electron transfer (eq 2) and spin transition (eq 3) steps that

$$\underset{(d\pi)^6(d\sigma)^0(\pi_{Q1})^2(\pi_{Q2})^1}{Co^{III}(N\text{-}N)(SQ)(Cat)} \rightarrow \underset{(d\pi)^6(d\sigma)^1(\pi_{Q1})^1(\pi_{Q2})^1}{Co^{II}(N\text{-}N)(SQ)_2} \quad (2)$$

$$\underset{(d\pi)^6(d\sigma)^1(\pi_{Q1})^1(\pi_{Q2})^1}{Co^{II}(N\text{-}N)(SQ)_2} \rightarrow \underset{(d\pi)^5(d\sigma)^2(\pi_{Q1})^1(\pi_{Q2})^1}{Co^{II}(N\text{-}N)(SQ)_2} \quad (3)$$

convert low-spin Co(III) to high-spin Co(II) in a process that may be viewed as a charge-transfer-induced spin transition.

Equilibrium measurements on $Co(bpy)(3,5\text{-}DBQ)_2$ recorded in solution and in the solid state have provided thermodynamic parameters that are in agreement with values for intramolecular

⊗ Abstract published in *Advance ACS Abstracts,* December 15, 1996.

(1) (a) Korea Institute of Science and Technology. (b) University of Colorado.
(2) (a) Gilat, S. L.; Kawai, S. H.; Lehn, J.-M. *Chem. Eur. J.* **1995**, *1*, 275. (b) Kawai, S. H.; Gilat, S. L.; Ponsinet, R.; Lehn, J.-M. *Chem. Eur. J.* **1995**, *1*, 285.
(3) Irie, M. In *Photoreactive Materials for Ultrahigh Density Optical Memory*; Irie, M., Ed.; Elsevier: Amsterdam, 1994; p 1.
(4) Kahn, O.; Kröber, J.; Jay, C. *Adv. Mater.* **1992**, *4*, 718.
(5) Gütlich, P.; Hauser, A.; Spiering, H. *Angew. Chem., Int. Ed. Engl.* **1994**, *33*, 2024.
(6) Goulle, V.; Harriman, A.; Lehn, J.-M. *J. Chem. Soc., Chem. Commun.* **1993**, 1034.
(7) Buchanan, R. M.; Pierpont, C. G. *J. Am. Chem. Soc.* **1980**, *102*, 4951.
(8) (a) Jung, O.-S.; Pierpont C. G. *J. Am. Chem. Soc.* **1994**, *116*, 1127. (b) Jung, O.-S.; Pierpont, C. G. *Inorg. Chem.* **1994**, 33, 2227.
(9) (a) Abakumov, G. A.; Cherkasov, V. K.; Bubnov, M. P.; Ellert, O. G.; Dobrokhotova, Z. B.; Zakharov, L. N.; Struchkov, Yu. T. *Dokl. Akad. Nauk* **1993**, *328*, 12. (b) Adams, D. M.; Dei, A.; Rheingold, A. L.; Hendrickson, D. N. *J. Am. Chem. Soc.* **1993**, *115*, 8221.

S0020-1669(96)01214-1 CCC: $14.00

enthalpy and entropy changes associated with Co(II)/Co(III) redox reactions.[10,11] Population of the antibonding dσ orbital results in a relatively large enthalpic increase that is primarily associated with destabilization of metal−ligand bonds. Associated low-energy shifts in vibrational modes with increases in complex spin degeneracy and structural flexibility give a large positive entropy change that is responsible for the strong temperature dependence of the equilibrium.[10] Together, these thermodynamic changes define the transition temperature (Tc) for the equilibrium. The Co(III) redox isomers exhibit intense electronic transitions in the infrared near 4000 cm^{-1}.[8] The nature of these transitions has not been established experimentally, but indirect evidence points to an assignment as the Cat → Co(III) charge-transfer band leading to the shift in charge distribution.[12]

The coupled metal−quinone redox chemistry, the potential for light-induced electron transfer, and the associated changes in spectral, structural, and magnetic properties combine to make the cobalt−quinone complexes uniquely well-suited for optical switching applications. Compounds that have been reported previously tend to show abrupt Co(III)/Co(II) transitions; no complex of the series has yet been found to exhibit reversible transition steps with significant thermal hysteresis. In the present report we describe studies on redox isomerism for the series of compounds prepared with the bis(pyridine) ether coligand and its heteroatomic thio-, seleno-, and telluroether analogs.

Experimental Section

Materials. 3,6-Di-*tert*-butyl-1,2-benzoquinone (3,6-DBBQ), 2,2′-bis(pyridine) ether (py_2O), 2,2′-bis(pyridine) thioether (py_2S), 2,2′-bis(pyridine) selenoether (py_2Se), and 2,2′-bis(pyridine) telluroether (py_2Te) were prepared by literature procedures.[13−17]

Co(py_2O)(3,6-DBQ)$_2$. $Co_2(CO)_8$ (86 mg, 0.25 mmol) and py_2O (86 mg, 0.50 mmol) were combined in 30 mL of toluene under an atmosphere of Ar. The mixture was stirred for 5 min, and 3,6-DBBQ (220 mg, 1.00 mmol) dissolved in 30 mL of toluene was added. The solution was stirred for 2 h at room temperature. Evaporation of the solvent gave the dark green microcrystalline product in 70% yield (235 mg). Dark blue crystals of Co(py_2O)(3,6-DBSQ)(3,6-DBCat) suitable for crystallographic characterization were obtained by recrystallization from acetone. Dark green crystals of Co(py_2O)(3,6-DBSQ)$_2$ were obtained by recrystallization from toluene. Anal. Calcd for $C_{38}H_{48}N_2O_5Co$: C, 67.86; H, 7.04; N, 4.13. Found: C, 67.95; H, 7.20; N, 4.17.

Co(py_2X)(3,6-DBQ)$_2$, X = S, Se, Te. Procedures used in the syntheses of these complexes were similar to those described above with equivalent quantities of the thio-, seleno-, and telluroether ligands used in place of py_2O. Co(py_2S)(3,6-DBQ)$_2$ was obtained in 82% yield. Anal. Calcd for $C_{38}H_{48}N_2O_4SCo$: C, 66.29; H, 6.84; N, 3.96. Found: C, 66.36; H, 7.03; N, 4.07. Co(py_2Se)(3,6-DBQ)$_2$ and Co(py_2Te)(3,6-DBQ)$_2$ were obtained in 68% and 62% yield. Recrystallization from acetone gave products as unstable acetone solvates with erratic elemental analyses, and the composition of these complexes was assigned on the basis of their spectroscopic and magnetic properties.

Table 1. Crystallographic Data for $Co^{III}(py_2O)(3,6\text{-DBSQ})(3,6\text{-DBCat})$ and $Co^{II}(py_2O)(3,6\text{-DBSQ})_2$

	Co(py_2O)(3,6-DBSQ)(3,6-DBCat)	Co(py_2O)(3,6-DBSQ)$_2$
formula	$C_{38}H_{48}N_2O_5Co$	$C_{38}H_{48}N_2O_5Co$
fw	671.71	671.71
color	dark blue	dark blue-green
space group	$P2_1/n$	$P2_1/c$
a (Å)	9.882(3)	11.0280(2)
b (Å)	20.915(5)	30.2750(9)
c (Å)	17.579(4)	12.1120(2)
β (deg)	91.57(2)	113.490(2)
V (Å^3)	3632(2)	3708.7(1)
Z	4	4
T (°C)	20	22
λ (Mo Kα, Å)	0.710 73	0.710 69
ρ_{calcd} (g cm^{-3})	1.228	1.203
μ (mm^{-1})	0.515	0.505
R, R_w	0.054, 0.105[a]	0.056, 0.053[b]

[a] $R = \Sigma||F_o| - |F_c||/\Sigma|F_o|$; $R_w = [\Sigma w(|F_o| - |F_c|)^2/\Sigma w|F_o|^2]^{1/2}$. [b] $R = \Sigma||F_o| - |Fc||/\Sigma|F_o|$; $R_w = [\Sigma w(F_o^2 - F_c^2)^2/\Sigma wF_o^4]^{1/2}$.

Physical Measurements. Electronic spectra were recorded on a Perkin-Elmer Lambda 9 spectrophotometer equipped with a RMC-Cyrosystems cryostat. Magnetic measurements were made using a Quantum Design SQUID magnetometer at a field strength of 5 kG. Infrared spectra were recorded on a Perkin-Elmer 1600 FTIR with samples prepared as KBr disks.

Crystallographic Structure Determinations. Co(py_2O)(3,6-DBSQ)(3,6-DBCat). Dark blue crystals of the complex were grown from acetone. Crystals form in the monoclinic crystal system, space group $P2_1/n$, in a unit cell of the dimensions given in Table 1. Intensity data were measured on an Enraf Nonius CAD-4 diffractometer within the angular range in Θ of 1.95−25.00°. The Co atom was located on a sharpened Patterson map, and phases generated from the location of the metal gave the positions of other atoms of the structure. Final cycles of refinement converged with discrepancy indices of $R = 0.054$ and $R_w(F^2) = 0.105$. Tables containing a full listing of atom positions, anisotropic displacement parameters, and hydrogen atom locations are available as Supporting Information.

Co(py_2O)(3,6-DBSQ)$_2$. Dark green crystals were obtained by recrystallization from toluene at room temperature. Crystals form in the monoclinic crystal system, space group $P2_1/c$, in a unit cell of the dimensions listed in Table 1. Intensity data were measured on a Rigaku R-AXIS II diffractometer at the Molecular Structure Corporation. Of the 15 563 reflections measured, 5370 were unique ($R_{int} = 0.046$) and used in the structure determination and refinement. The structure was solved using the Fourier methods contained in DIRDIF94. Final cycles of refinement converged with discrepancy indices of $R = 0.056$ and $R_w = 0.053$. Tables containing a full listing of atom positions, anisotropic displacement parameters, and hydrogen atom locations are available as Supporting Information.

Results

Equilibria between cobalt−quinone redox isomers have been found to be extremely sensitive to the properties of nitrogen-donor coligands. The solid-state transition temperature of Co(tmeda)(3,6-DBQ)$_2$ is 200 K higher than the related complex prepared with *N*,*N*,*N*′,*N*′-tetramethylpropylenediamine (tmpda).[18] The addition of a single methylene group to the chelate ring of the coligand has a dramatic effect on cobalt−quinone electron transfer. The present investigation has been carried out to study the effects of coligand composition and structure for complexes containing bis(pyridine) ether (**I**) and its sulfur, selenium, and tellurium analogs. Properties of complexes prepared with the X = S, Se, and Te series are similar; the py_2O complex will be described separately.

(10) Pierpont, C. G.; Jung, O.-S. *Inorg. Chem.* **1995**, *34*, 4281.
(11) (a) Richardson, D. E.; Sharpe, P. *Inorg. Chem.* **1991**, *30*, 1412. (b) Richardson, D. E.; Sharpe, P. *Inorg. Chem.* **1993**, *32*, 1809. (c) Crawford, P. W.; Schultz, F. A. *Inorg. Chem.* **1994**, *33*, 4344. (d) Gao, Y.-D.; Lipkowitz, K. P.; Schultz, F. A. *J. Am. Chem. Soc.* **1995**, *117*, 11932.
(12) Jung, O.-S.; Pierpont, C. G. *J. Am. Chem. Soc.* **1994**, *116*, 2229.
(13) Belostotskaya, I. S.; Komissarova, N. L.; Dzhuaryan, E. V.; Ershov, V. V. *Izv. Akad. Nauk SSSR* **1972**, 1594.
(14) de Villiers, P. A.; den Hertog, H. J. *Recl. Trav. Chim. Pays-Bas* **1957**, *76*, 647.
(15) Chachaty, C.; Pappalardo, G. C.; Searlata, G. *J. Chem. Soc., Perkin Trans. 2* **1976**, 1234.
(16) Grant, H. G.; Summers, L. A. *Z. Naturforsh.* **1978**, *33B*, 118.
(17) Dunne, S. J.; Summers, L. A.; von Nagy-Felsobuki, E. I. *J. Heterocycl. Chem.* **1993**, *30*, 409.
(18) Jung, O.-S.; Jo, D. H.; Lee, Y.-A; Sohn, Y. S.; Pierpont, C. G. *Angew. Chem., Int. Ed. Engl.* **1996**, *35*, 1694.

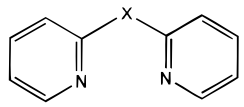

X = O, S, Se, Te

(I)

$Co(py_2X)(3,6\text{-}DBQ)_2$, X = S, Se, Te Synthetic procedures described in earlier studies have been used to prepare members of the $Co(N\text{-}N)(3,6\text{-}DBQ)_2$ series with the heteroatomic bis-(pyridine) ether ligands. Spectral and magnetic measurements on the three complexes prepared with the thio-, seleno-, and telluroether ligands have been used to monitor the equilibrium between low-spin Co(III) and high-spin Co(II) redox isomers (eq 1). It was anticipated, on the basis of values for atomic radius and electronegativity, that the complexes containing S and Se would be similar, with a small change in Tc for the Te complex. It was surprising to find the dramatic shifts shown in Figure 1. At temperatures below 150 K all three complexes are in the $Co^{III}(py_2X)(3,6\text{-}DBSQ)(3,6\text{-}DBCat)$ isomeric form with $S = {}^1/_2$ magnetic moments due to the radical semiquinone ligand. As sample temperature is increased, shifts to the high-spin $Co^{II}(py_2X)(3,6\text{-}DBSQ)_2$ redox isomer are observed with transition temperatures of 370, 290, and 210 K for the ligands containing S, Se, and Te bridging atoms, respectively. Magnetic moments for the $Co^{II}(py_2X)(3,6\text{-}DBSQ)_2$ isomers reflect the effects of magnetic exchange between the radical ligands and the paramagnetic S = 3/2 metal ion. There appears to be a pattern for the S, Se, and Te series that the complexes with higher transition temperatures have the largest magnetic moments for the Co(II) isomers. Differences in the strength of Co−SQ antiferromagnetic exchange contribute to variations in the extent to which high-order spin states are populated.

In toluene solution a similar pattern is observed from intensity changes in characteristic spectral bands. In all four cases, the Co(III) redox isomer has an intense transition near 600 nm, while the Co(II) isomer has two overlapped transitions centered near 850 nm (Table 2). The Co(III) isomers also have characteristic absorptions in the 1600−1700 nm region of the NIR and a strong band in the 2400−2600 nm region of the infrared. Temperature dependent changes in the intensity of visible transitions have been used to obtain transition temperatures of 255, 225, and <200 K for the S, Se, and Te series in toluene solution. Transition temperatures change in increments of approximately 80 K for the series in the solid state and in increments of 30 K in toluene solution. Measurements made in more polar solvents show a general increase in Tc with solvent polarity following observations made earlier for complexes prepared with a variety of different coligands.[8] Differences in Tc for members of the py_2X series are striking given the anticipated similarity in the coordination properties of the pyridine nitrogen atoms.

$Co(py_2O)(3,6\text{-}DBQ)_2$ Temperature dependent changes in optical spectra have been used to determine that the transition temperature for $Co^{III}(py_2O)(3,6\text{-}DBSQ)(3,6\text{-}DBCat)$ in toluene solution is approximately 250 K, close to the value for the thioether complex. In acetone solution Tc is higher, 280 K, but at room temperature in both solvents the complex is mainly in the form of the Co(II) redox isomer. Crystals grown from the two solvents show markedly different spectral and magnetic properties that indicate a change in charge distribution. Crystallographic characterization on crystals obtained from toluene has shown that the sample contains the $Co^{II}(py_2O)(3,6\text{-}DBSQ)_2$ redox isomer. A view of the molecule is shown in Figure 2; selected bond lengths and angles are listed in Table 3. Structural changes associated with the transition from low-spin Co(III) to high-spin Co(II) have been reviewed and appear primarily as large increases in Co−O,N bond lengths due to the addition of charge to the antibonding dσ orbital of the metal.[8,9] Smaller changes in ligand features are observed with the transfer of charge to the metal and the oxidation of one ligand from Cat to SQ. The py_2O ligand of $Co(py_2O)(3,6\text{-}DBSQ)_2$ is essentially planar, including the bridging ether oxygen atom. This permits

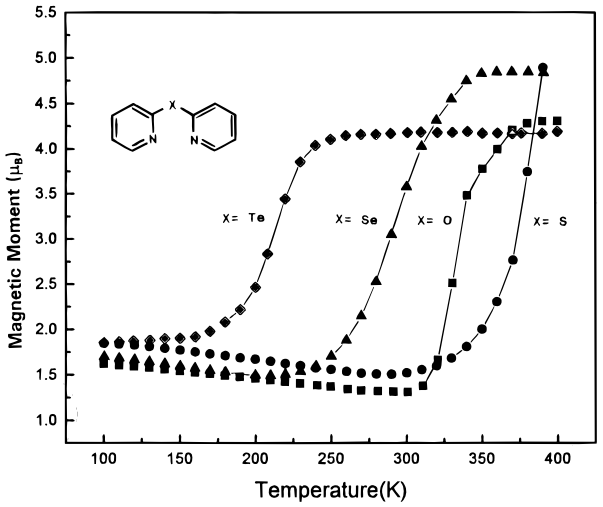

Figure 1. Magnetic measurements on complexes of the $Co(py_2X)(3,6\text{-}DBQ)_2$ series with X = S (●), Se (▲), and Te (◆), and on a sample of $Co(py_2O)(3,6\text{-}DBQ)_2$ (■) recrystallized from acetone.

Table 2. Electronic Spectral Bands and Transition Temperatures (Tc) for Members of the $Co(py_2X)(3,6\text{-}DBQ)_2$ Series

	UV−vis−near-IR (nm, log ϵ)[a]		Tc (K)	
X	Co(III)	Co(II)	solid	toluene
O	600 (3.7), 1700 (3.4), 2400	740 (3.4), 825 (sh)	110, 330[b]	250
S	605 (3.7), 1600 (3.2), 2400	740 (3.4), 830 (sh)	370	255
Se	600 (3.6), 1700 (3.2), 2550	750(3.3), 820(sh)	290	225
Te	600(3.7), 1650(3.2), 2600	750(3.3), 830(sh)	210	<200

[a] Spectra recorded either in toluene solution or as solid KBr pellets. Molar extinction coefficients are expressed in units of M^{-1} cm^{-1}. [b] Values for Tc↓ and Tc↑ for samples obtained by recrystallization from acetone.

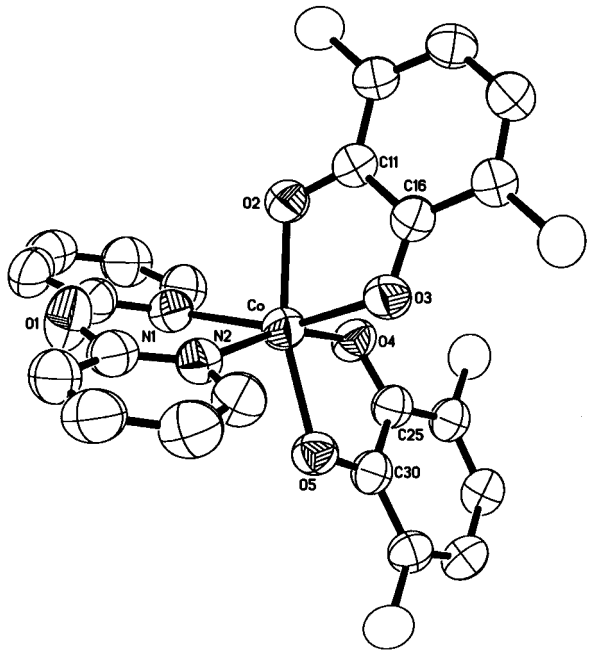

Figure 2. View of the $Co^{II}(py_2O)(3,6\text{-}DBSQ)_2$ molecule obtained by recrystallization from toluene.

Table 3. Selected Bond Lengths and Angles for $Co^{II}(py_2O)(3,6\text{-}DBSQ)_2$ and $Co^{III}(py_2O)(3,6\text{-}DBSQ)(3,6\text{-}DBCat)$

	$Co^{II}(py_2O)$-$(3,6\text{-}DBSQ)_2$	$Co^{III}(py_2O)$-$(3,6\text{-}DBSQ)(3,6\text{-}DBCat)$[a]
	Bond Lengths (Å)	
Co−O2	2.029(3)	1.841(4)
Co−O3	2.067(3)	1.847(4)
Co−O4	2.065(3)	1.890(4)
Co−O5	2.037(3)	1.892(4)
Co−N1	2.133(4)	1.926(6)
Co−N2	2.126(4)	1.956(6)
$C-O_{SQ}$	1.280(4)	1.293(6)
$C-O_{Cat}$		1.360(7)
	Angles (deg)	
O2−Co−O3	78.1(1)	87.9(2)
O4−Co−O5	78.0(1)	85.7(2)
N1−Co−N2	85.1(2)	89.0(3)
C5−O1−C6	130.7(4)	122.8(7)

[a] Oxygen atoms O2 and O3 of $Co^{III}(py_2O)(3,6\text{-}DBSQ)(3,6\text{-}DBCat)$ belong to the catecholate ligand (Figure 5).

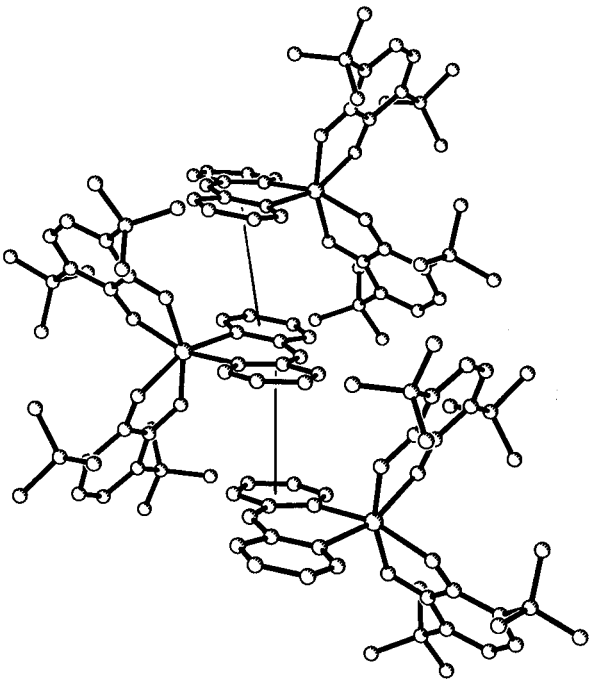

Figure 3. View showing intermolecular stacking for the crystal structure of $Co^{II}(py_2O)(3,6\text{-}DBSQ)_2$.

intermolecular stacking between pyridine rings of adjacent complex molecules to give the slipped columnar crystal structure shown in Figure 3. Magnetic measurements have been made on samples of $Co^{II}(py_2O)(3,6\text{-}DBSQ)_2$ obtained from toluene solution with the result shown in Figure 4. The magnetic moment remains in the range between 3.5 and 4.0 μ_B down to 20 K. Below 20 K, the moment drops as a probable consequence of contributions from weak intermolecular magnetic exchange. Transition temperatures for the Co(III)/Co(II) shift in charge distribution are typically higher in the solid-state than in solution. In this case the solid state structure appears to surpress the low-temperature transition to $Co^{III}(py_2O)(3,6\text{-}DBSQ)(3,6\text{-}DBCat)$ for samples obtained by recrystallization from toluene.

Recrystallization from acetone gives $Co^{III}(py_2O)(3,6\text{-}DBSQ)(3,6\text{-}DBCat)$ in the solid state at room temperature. A view of the molecule is shown in Figure 5; selected bond lengths and angles are listed in Table 3. The radius of low-spin Co(III) is roughly 0.2 Å shorter than the radius of high-spin Co(II), and this difference appears as a contraction in the Co−O,N bond

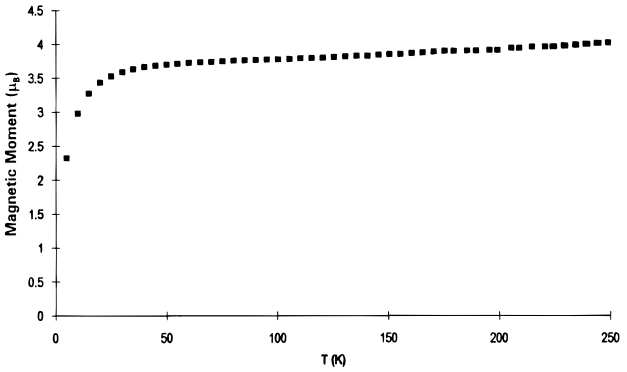

Figure 4. Magnetic measurements made on a sample of $Co^{II}(py_2O)(3,6\text{-}DBSQ)_2$ obtained by recrystallization from toluene.

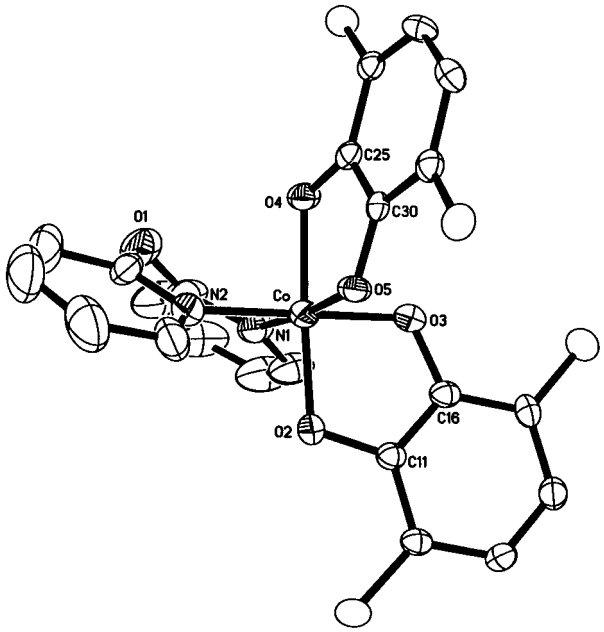

Figure 5. View of the $Co^{III}(py_2O)(3,6\text{-}DBSQ)(3,6\text{-}DBCat)$ molecule obtained by recrystallization from acetone.

lengths relative to the values of the Co(II) isomer. Further, structural features of the quinone ligands of $Co(py_2O)(3,6\text{-}DBSQ)(3,6\text{-}DBCat)$ show that one is a localized semiquinonate and the other a catecholate with longer C−O lengths and aromatic ring C−C lengths. A striking and significant feature of the molecule is the folded structure of the py_2O ligand. This appears to result from structural constraints imposed by the decrease in Co-N bond lengths, from an average value of 2.130(4) Å for the Co(II) redox isomer to 1.941(6) Å for $Co^{III}(py_2O)(3,6\text{-}DBSQ)(3,6\text{-}DBCat)$. The fold results in a N-Co-N bond angle of 89.0(3)°, close to 90°, and contraction in the C−O−C angle at the ether oxygen to 122.8(7)°, relative to the angle of 130.7(4)° for the planar ligand of the Co(II) isomer. The dihedral angle between planes of py_2O pyridine rings is 36° for the Co(III) isomer; for $Co^{II}(py_2O)(3,6\text{-}DBSQ)_2$ the angle is less than 7°, and the folded structure prevents intermolecular stacking of the type found for the Co(II) isomer. The closest intermolecular contact shown in Figure 6 is between oxygen atoms of adjacent molecules at a distance of 4.19 Å.

Hysteresis in Magnetic Measurements The results of temperature dependent magnetic measurements recorded on a sample of $Co^{III}(py_2O)(3,6\text{-}DBSQ)(3,6\text{-}DBCat)$ obtained from acetone solution are shown in Figure 1. The transition temperature for this sample is near 330 K, and the magnetic moment for the Co(II) isomer formed is 4.3 μ_B.

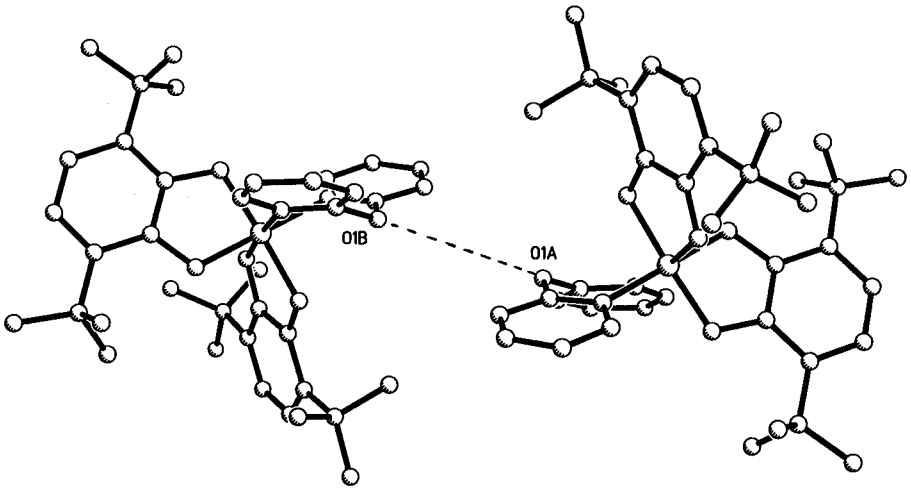

Figure 6. View showing the closest intermolecular separation (4.19 Å) between ether oxygen atoms of $Co^{III}(py_2O)(3,6\text{-}DBSQ)(3,6\text{-}DBCat)$.

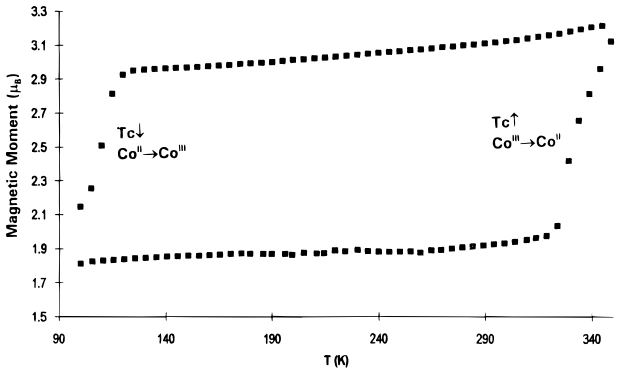

Figure 7. Hysteresis for magnetic measurements on $Co(py_2O)(3,6\text{-}DBQ)_2$. The measurement shown was obtained by starting at 100 K on a sample of the Co(III) isomer obtained from acetone.

The difference in magnetic behavior for samples of the complex obtained from toluene and acetone is striking. Neither of the redox isomers is obtained as a solvate, and differences in solid-state electron transfer properties are associated with intermolecular interactions that occur within the lattice. The constrained planarity of the py_2O ligand creates a high-energy barrier to electron transfer for the Co(II) isomer, and the complex fails to shift to the Co(III) form. Lattice effects contribute to the thermal hysteresis observed for spin transition complexes that are of interest as molecular switches. To investigate this property for the Co(III) isomer obtained from acetone, measurements in magnetic moment were made by scanning over the temperature range between 50 and 340 K. The plot of μ_B vs T for one cycle is shown in Figure 7. At high temperature the Co(III) → Co(II) transition takes place with a $Tc\uparrow$ of 330 K, but the reverse transition, Co(II) → Co(III), is observed to occur with a $Tc\downarrow$ near 100 K. Thermal hysteresis is observed with a temperature difference of approximately 230 K between steps. The observation that the Co(II) isomer formed at high temperature shifts back to the Co(III) isomer at a lower temperature indicates that the solid-state environment of the Co(II) complex formed by the shift at 330 K is different from the stacked structure found for the form of the Co(II) isomer obtained by recrystallization from toluene. Repeated cycling over the hysteresis loop reveals that with rapid changes in temperature the switching effect is essentially reversible. However, slow changes in sample temperature result in a decrease in $Tc\uparrow$ with gradual loss in reversibility of the switching effect. Recrystallization of the sample from acetone restores hysteresis, and there is little decomposition of the complex during the cycle.

Optical Switching It may be possible to convert the metastable Co(III) isomer formed by recrystallization from acetone to the Co(II) isomer by optical excitation on the Cat → Co(III) charge-transfer transition at a temperature below $Tc\uparrow$. This offers an opportunity to investigate optical switching properties, and it also permits study of the energy dependence of charge transfer. Experiments have been carried out on samples of the Co(III) isomer prepared as a KBr disk. The optical spectrum of the sample is shown in Figure 8. The intense transition at 600 nm appears characteristically for the Co(III) isomers of the Co(N-N)(DBSQ)(DBCat) complexes, and recent excited-state lifetime studies by Hendrickson and Simon have demonstrated the LMCT nature of this transition.[19] The lifetime of this excited state is short, and its relationship to the change in charge distribution that leads to redox isomerism remains in question. To investigate this relationship a KBr disk containing $Co^{III}(py_2O)(3,6\text{-}DBSQ)(3,6\text{-}DBCat)$ was irradiated with a 10 mW He/Ne laser at a wavelength of 633 nm. No change in the optical spectrum of the sample was observed. The same sample was irradiated briefly with light from a polychromatic tungsten lamp, and the spectrum was observed to shift to that of $Co^{II}(py_2O)(3,6\text{-}DBSQ)_2$ (Figure 8). These experiments were carried out with the sample cooled to approximately 270 K with a stream of cold N_2 to minimize the effects of thermal electron transfer. However, this experiment fails to demonstrate that electron transfer occurs optically; studies on wavelength sensitivity are in progress over the region between 1700 and 3000 nm.

Discussion

Structural characterizations on several complexes containing the py_2S ligand have shown that it has a folded structure, even in cases where M−N bond lengths are close to the coligand Co-N lengths of the Co(II) isomers.[20] It is, therefore, reasonable to assume that the py_2X ligands of both the Co(II) and Co(III) redox isomers with X = S, Se, and Te are nonplanar, and there is little change in coligand structure with the shift in charge distribution. Transition temperatures for redox isomerism vary in steps of 30 K intervals in toluene solution and 80 K intervals

(19) Adams, D. M.; Li B.; Simon, J. D.; Hendrickson, D. N. *Angew. Chem., Int. Ed. Engl.* **1995**, *34*, 1481.
(20) (a) Kondo, M.; Kawata, S.; Kitagawa, S.; Kiso, H.; Munakata, M. *Acta Crystallogr., Sect. C* **1995**, *51*, 567. (b) Tresoldi, G.; Rotondo, E.; Piraino, P.; Lanfranchi, M.; Tiripicchio, A. *Inorg. Chim. Acta* **1992**, *194*, 233. (c) De Munno, G.; Bruno, G.; Rotondo, E.; Giordano, G.; Lo Schiavo, S.; Piraino, P.; Tresoldi, G. *Inorg. Chim. Acta* **1993**, *208*, 67.

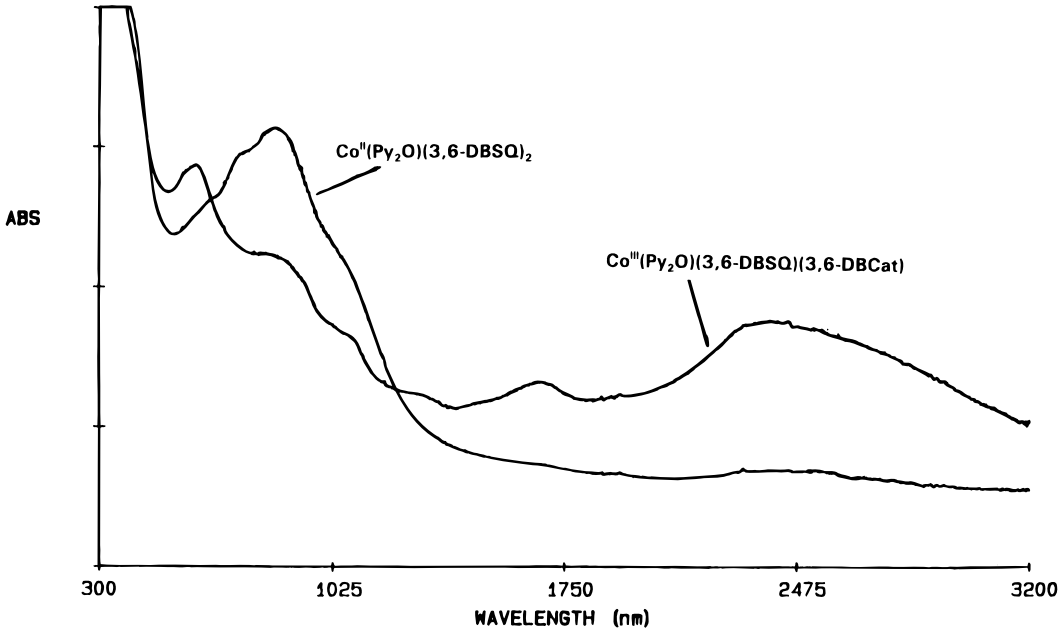

Figure 8. Changes in optical spectrum upon irradiation of a KBr disk containing Co(py$_2$O)(3,6-DBSQ)(3,6-DBCat) for the period of several seconds.

in the solid state for the S, Se, and Te series. This is not the pattern that would be expected for an effect associated with changes in heteroatom radius or electronegativity, but it roughly follows the pattern of changes in atomic mass. Transition temperature is defined by the ratio of enthalpy and entropy changes for the Co(III)/Co(II) equilibrium. Solid-state structures of complexes prepared with the three heteroethers are probably similar, the donor character of the pyridine nitrogen atoms is not very different for the series, and enthalpy changes for the three equilibria associated with changes in Co−N bond energy are probably similar. Studies on entropic contributions to Co(III)/Co(II) redox equilibria show that low-frequency shifts in vibrational modes result in dramatic increases in entropy change. The mass increase with the change in py$_2$X heteroatom, from sulfur to tellurium, decreases the energy of vibrational modes associated with the py$_2$X ligand. The resulting increase in ΔS may be responsible for the progressive decrease in Tc with increasing heteroatomic mass.

The complex prepared with the bis(pyridine) ether ligand py$_2$O is anomalous, and this difference seems related to the planar/folded shift in structure with metal charge, spin state, and radius. Co^{II}(py$_2$O)(3,6-DBSQ)$_2$ obtained by recrystallization from toluene is locked into the Co(II) charge distribution by restrictions placed on the py$_2$O ligand by the layered structure. The ligand cannot switch to the folded structure of the Co(III) isomer without a significant disruption of the solid-state lattice. The open crystal structure of Co^{III}(py$_2$O)(3,6-DBSQ)(3,6-DBCat) (Figure 6) permits conformational shifts in coligand structure, allowing the metal to undergo shifts in charge distribution that appear as differences in magnetic properties, but with significant hysteresis between forward and reverse electron transfer steps.

The environment of the py$_2$O coligand seems responsible for differences in Co−quinone electron transfer and redox isomerism for forms of the complex obtained by recrystallization from different solvent media. The arrangement of Co^{II}(py$_2$O)(3,6-DBSQ)$_2$ molecules formed by Cat → Co(III) electron transfer from Co^{III}(py$_2$O)(3,6-DBSQ)(3,6-DBCat) in the solid state would differ from the crystal structure of samples obtained by toluene recrystallization. Stacking interactions of the type shown in Figure 3 occur commonly for similar complexes containing polypyridine coligands.[7,8] Repeated cycling over the hysteresis loop shown in Figure 7 results in a gradual decrease in Tc↑ with loss of reversibility. This may be associated with regional stacking of Co(II) isomers, a progressive shift in solid-state lattice structure to that shown in Figure 3, and irreversible formation of the Co(II) redox isomer.

Conclusions

Strong intermolecular interactions have been viewed as important in creating cooperative, path-dependent physical changes that may be useful in switching applications.[4,5] Intermolecular stacking inhibits electron transfer for Co^{II}(py$_2$O)(3,6-DBSQ)$_2$, but a relatively weak intermolecular response to shifts in charge distribution and structure in the lattice of Co^{III}(py$_2$O)(3,6-DBSQ)(3,6-DBCat) creates a dramatic hysteresis effect. Switching properties appear to be associated with the planar/folded change in conformation of the py$_2$O ligand associated with electron transfer between the metal and quinone ligands.

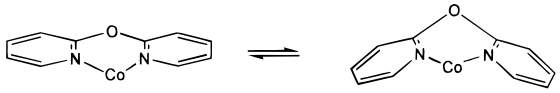

Co^{II}(py$_2$O)(3,6-DBSQ)$_2$ Co^{III}(py$_2$O)(3,6-DBSQ)(3,6-DBCat)

Acknowledgment. Research carried out at KIST was supported as part of the E-project through Grant 2N13694. Research at the University of Colorado was supported by the National Science Foundation. We would like to thank Dr. Beverly Vincent and Dr. Catherine Day of the Molecular Structure Corporation for help with the structure determination on Co(py$_2$O)(3,6-DBSQ)$_2$.

Supporting Information Available: Details of the structure determinations on Co^{III}(py$_2$O)(3,6-DBSQ)(3,6-DBCat) and Co^{II}(py$_2$O)(3,6-DBSQ)$_2$ (28 pages). Ordering information is given on any current masthead page.

IC961214D